ARTICLE

BIOTECHNOLOGY and BIOENGINEERING

Naringenin-Responsive Riboswitch-Based Fluorescent Biosensor Module for *Escherichia coli* Co-Cultures

Yu Xiu,[1,2,3] Sungho Jang,[4] J. Andrew Jones,[3,5] Nicholas A. Zill,[3] Robert J. Linhardt,[3] Qipeng Yuan,[1] Gyoo Yeol Jung ,[4,6] Mattheos A. G. Koffas [3]

[1]State Key Laboratory of Chemical Resource Engineering, Beijing University of Chemical Technology, Beijing, China

[2]Beijing Key Laboratory of Bioactive Substances and Functional Food, Beijing Union University, Beijing, China

[3]Department of Chemical and Biological Engineering, Center for Biotechnology and Interdisciplinary Studies, Rensselaer Polytechnic Institute, Troy, New York; telephone: (518) 276-2220; fax: (518) 276-3405; e-mail: koffam@rpi.edu

[4]Department of Chemical Engineering, Pohang University of Science and Technology, Pohang, Gyeongbuk, Korea

[5]Department of Chemistry, Hamilton College, Clinton, New York

[6]School of Interdisciplinary Bioscience and Bioengineering, Pohang University of Science and Technology, Pohang, Gyeongbuk, Korea

ABSTRACT: The ability to design and construct combinatorial synthetic metabolic pathways has far exceeded our capacity for efficient screening and selection of the resulting microbial strains. The need for high-throughput rapid screening techniques is of upmost importance for the future of synthetic biology and metabolic engineering. Here we describe the development of an RNA riboswitch-based biosensor module with dual fluorescent reporters, and demonstrate a high-throughput flow cytometry-based screening method for identification of naringenin over producing *Escherichia coli* strains in co-culture. Our efforts helped identify a number of key operating parameters that affect biosensor performance, including the selection of promoter and linker elements within the sensor-actuator domain, and the effect of host strain, fermentation time, and growth medium on sensor dynamic range. The resulting biosensor demonstrates a high correlation between specific fluorescence of the biosensor strain and naringenin titer produced by the second member of the synthetic co-culture system. This technique represents a novel application for synthetic microbial co-cultures and can be expanded from naringenin to any metabolite if a suitable riboswitch is identified. The co-culture technique presented here can be applied to a variety of target metabolites in combination with the SELEX approach for aptamer design. Due to the compartmentalization of the two genetic constructs responsible for production and detection into separate cells and application as independent modules of a synthetic microbial co-culture we have subsequently reduced the need for re-optimization of the producer module when the biosensor is replaced or removed.

Biotechnol. Bioeng. 2017;114: 2235–2244.

KEYWORDS: riboswitch; co-culture; RNA aptamer; naringenin; flow cytometry; flavonoids; biosensor design

Conflicts of interest: The authors declare no conflicts of interest.
Correspondence to: M.A.G. Koffas
Contract grant sponsor: National Research Foundation of Korea
Contract grant numbers: NRF-2015R1A2A1A10056126; NRF-2016K1A1A2912829
Contract grant sponsor: National Natural Science Foundation of China
Contract grant number: 21376017
Received 25 April 2017; Revision received 11 May 2017; Accepted 16 May 2017
Accepted manuscript online 20 May 2017;
Article first published online 5 June 2017 in Wiley Online Library (http://onlinelibrary.wiley.com/doi/10.1002/bit.26340/abstract).
DOI 10.1002/bit.26340

Introduction

Riboswitches are common RNA-based genetic units that can regulate, either by inhibiting or activating, the expression of certain metabolic genes on pre-transcriptional, transcriptional, post-transcriptional, or translational levels through a variety of mechanisms, in response to the presence of a small molecule, without the need of proteins (Chang et al., 2012; Liu et al., 2015; Topp and Gallivan, 2010; Wachsmuth et al., 2013). Natural regulatory RNA riboswitches are found in a wide range of prokaryotes and are usually located in the untranslated regions of metabolic genes. Typically, riboswitches are composed of two domains: a sensing domain (an aptamer) and regulating domain (expression platform), generally functioning through allosteric control of gene-regulatory activity. Binding of a small molecule ligand to the aptamer domain causes a conformational change, which then results in modification of specific gene expression

(Liu et al., 2015; McKeague et al., 2016; Topp and Gallivan, 2010; Wachsmuth et al., 2013; Wittmann and Suess, 2012).

Systematic Evolution of Ligands by Exponential enrichment (SELEX) and its new enhancements(McKeague et al., 2016), Hi-Fi SELEX, single round SELEX, microfluidic SELEX, semi-automated SELEX, CE-SELEX, capture-SELEX, and branched SELEX, have allowed for the screening of new aptamers that respond to a plethora of natural and non-natural ligands. Riboswitches are therefore of great interest for understanding and reprogramming cellular behavior. However, aptamers isolated in vitro do not always retain activities under in vivo conditions, therefore a secondary screen or rational design of RNA devices must be performed. Several computer-aided design platforms were also developed to (i) identify sequence-structure motifs through SELEX (Alam et al., 2015; Hoinka et al., 2015); (ii) predict in vivo gene-regulatory activities through stochastic kinetic folding simulations (Carothers et al., 2011; Endoh and Sugimoto, 2015); (iii) perform massively parallel assays (Geertz et al., 2012; Townshend et al., 2015); and (iv) engineer complex sequence-structure-activity relationship of RNA devices that can process cellular information (Espah Borujeni et al., 2016).

Advances in generating synthetic riboswitches have accelerated their application as genetic controllers in the areas of molecular sensors, metabolic pathway optimization (Cress et al., 2015; Dietrich et al., 2010; Liu et al., 2015; McKeague et al., 2016; Rogers et al., 2016) and therapeutic applications (Davydova et al., 2016; Lee et al., 2016). In the past decade, several natural and artificial RNA-based sensors have been engineered to respond to a wide range of metabolites, including folinic acid (Trausch et al., 2011), theophylline (Beisel et al., 2011; Lynch et al., 2007; Michener and Smolke, 2012; Topp et al., 2010; Wachsmuth et al., 2013), xanthine (Beisel et al., 2011), tetracycline (Beisel et al., 2011; Weigand and Suess, 2007), ammeline (Dixon et al., 2010), cyclic-di-GMP (Kellenberger et al., 2015b; Lynch et al., 2007), cyclic-di-AMP (Kellenberger et al., 2015a), β-catenin (Bloom et al., 2014), thiamine 5′-pyrophosphate (TPP) (You et al., 2015), guanine (Paige et al., 2012; You et al., 2015), adenine (You et al., 2015), S-adenosyl-methionine (SAM) (Paige et al., 2012; You et al., 2015), adenosine 5-diphosphate (ADP) (Paige et al., 2012), guanosine 5-triphosphate (GTP) (Paige et al., 2012), flavin mononucleotide (FMN) (Meyer et al., 2015), lysine (Yang et al., 2013; Zhou and Zeng, 2015), glucosamine 6-phosphate (Lee and Oh, 2015) in prokaryotic, eukaryotic, and mammalian cells through various mechanisms.

Significant progress has been made in the biosynthesis of natural products such as flavonoids using a variety pathway optimization strategies (Cress et al., 2015, 2016; Jones et al., 2016; Pandey et al., 2016; Raman et al., 2014). Interest in flavonoids has emerged in recent years due to the potential clinical use of these compounds. (Bhan et al., 2013; Pandey et al., 2016; Thaiss et al., 2016; Wang et al., 2016) In order to develop screening methods for flavonoid producers, two natural naringenin-responsive transcription factors, FdeR from *Herbaspirillum serpedicae* SmR1 (Marin et al., 2013) and TtgR from *Pseudomonas putida* DOT-T1E (Terán et al., 2003), were identified. They were used in a FdeR-biosensor for intracellular detection of naringenin concentration (Siedler et al., 2014) and in a TtgR–TolC sensor-selector for screening of targeted genome-wide mutagenesis for naringenin high-producing strains (Raman et al., 2014). Here, we report the construction of an RNA riboswitch-based fluorescent biosensor using a novel synthetic aptamer that activates gene expression upon naringenin binding. The biosensor was characterized with different genetic components, in different strain backgrounds, and under different growth conditions in order to optimize its performance and better correlate naringenin input with reporter protein output. This represents the first example of a producer-biosensor co-culture system that has been developed and applied for product quantification. This process for biosensor design and characterization is useful in various applications, such as the dynamic regulation of naringenin-producing genetic circuits, and in high-throughput screening of natural or recombinant strains.

Results

A Naringenin-Responsive Riboswitch-Based Device as a Platform for In Vivo Naringenin Detection

Naringenin-responsive, single-stranded RNA was isolated from combinatorially prepared nucleic acid libraries using SELEX (submitted for publication). Using the previously identified naringenin-responsive RNA aptamer (Fig. 1B), four riboswitch sensing-actuation devices were constructed to detect, report, and act on environmental and intracellular signals. These devices are comprised of two modular subunits (Fig. 1A): (i) a riboswitch module, with an aptamer, for sensing the small molecule naringenin, and an actuator acting as a switch for downstream gene expression controlled by the metabolite-induced conformational change of the riboswitch module; (ii) a dual expression module (Yang et al., 2013): growth-based selection marker *tetA*, encoding a tetracycline/H^+ antiporter, and fluorescent reporter marker *sgfp*.

The aptamer O-, M1-, and M2- (Fig. 1B) mediated in vivo biosensor provided varied concentration-dependent responses to naringenin supplementation (Fig. 1C). Their responses were characterized by their dynamic range or signal-to-noise ratio (quantified as the ratio of a highest fluorescent signal in the presence of ligand to that in absence of ligand) (Rogers et al., 2016) and operational range (defined as the range of concentrations over which the biosensor exhibits a graded, concentration-dependent change in output fluorescent signal) (Rogers et al., 2016). The aptamer-M1-based biosensor demonstrated the highest dynamic range of approximately 4.9 (a.u.). The aptamer-O-based biosensor showed a dynamic range of about 3.7 (a.u.) and the aptamer-M2-based biosensor showed a dynamic range of about 2.4 (a.u.). However, aptamer-M2-based biosensor demonstrated the broadest operational range, from 0 to 0.6 mM naringenin, compared to the other two biosensors, which both displayed similar operational range up to 0.4 mM naringenin in culture.

The half maximal effective concentrations (EC_{50}) for the different aptamers, an indirect measure of binding affinity of the aptamer to naringenin, are illustrated in Figure 1C. The EC_{50} value of aptamer-M2-based biosensor was the largest and the EC_{50} of the aptamer-O-based biosensor slightly greater than the smallest EC_{50} observed for the aptamer-M1-based biosensor. The aptamer-H2-based biosensor, composed of the same aptamer as M2 but with different $(N)_{10}$

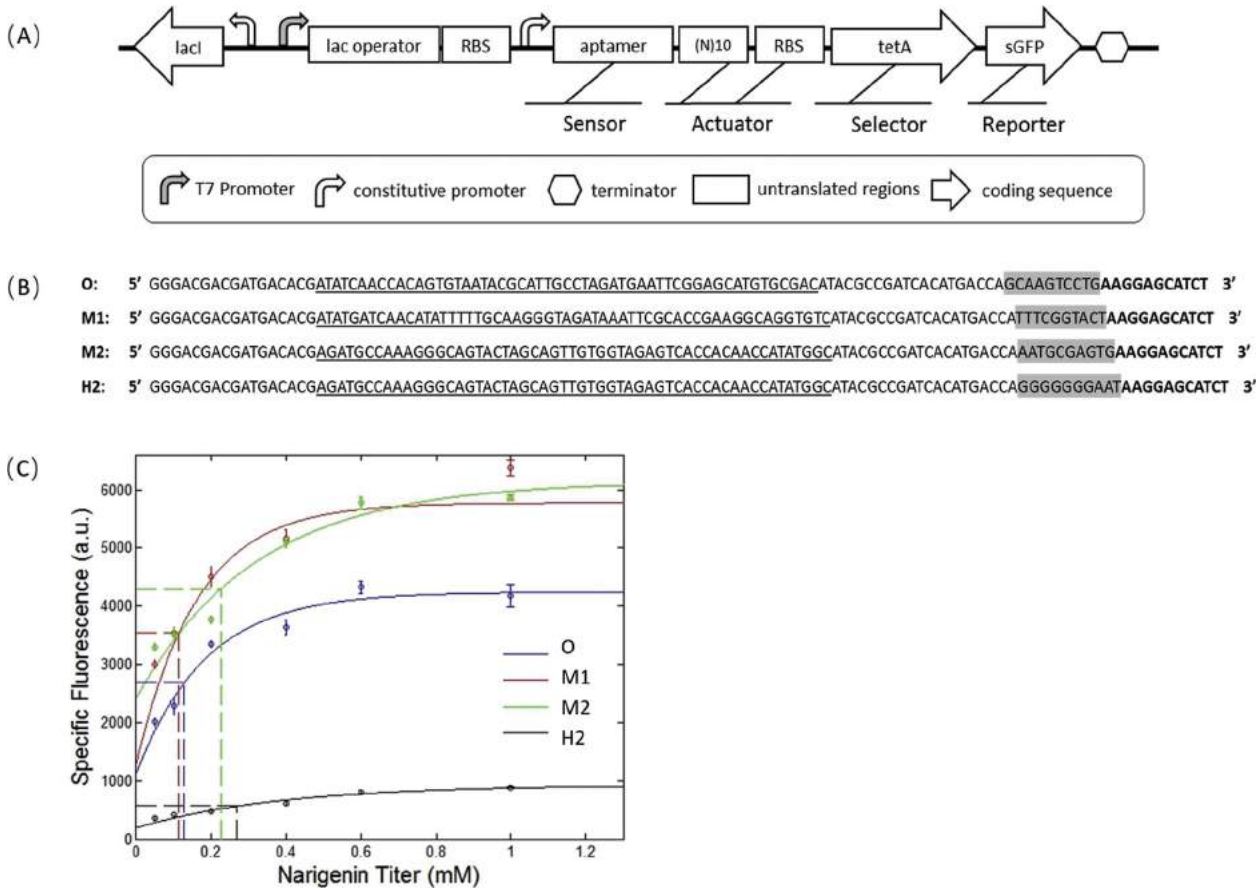

Figure 1. Naringenin-binding riboswitch devices construction and in vivo test. (**A**) Riboswitch sensing-actuation devices subunits. (**B**) Sequence of sensor and actuator of different riboswitches: O, M1, M2, H2. The binding domain (underlined) is located between a consensus noncoding upstream and downstream sequence, together composing the sensor part of riboswitch devices. Selected $(N)_{10}$ sequences are shown in shadow and the ribosomal binding site is shown in bold. (**C**) Effector range and response with different riboswitch devices single plasmid in BL21star™(DE3) detected by flow cytometry. The EC_{50} for the different aptamers are illustrated as dashed lines.

linkage sequences (Fig. 1B), showed a noticeable decrease of fluorescent protein output as a function of naringenin concentration compared to that of M2 (Fig. 1C).

A single plasmid riboswitch device was tested in two host strains, wild type BL21star™(DE3) and MG1655(DE3) Δ*endA* Δ*recA*, with different naringenin concentrations added at 0 h. The two hosts displayed significantly different dynamic ranges. When 0.73 mM naringenin was fed to aptamer-O-based biosensor, the fluorescence intensity per cell reached 4285 (a.u.) when expressed in BL21star™(DE3), but only 2884 (a.u.) when expressed in MG1655(DE3) Δ*endA* Δ*recA* (Fig. 2). Meanwhile, the fluorescence output for each naringenin concentration studied showed a steady increase until reaching saturation after approximately 12 h post inoculation in both wild type strains (Fig. 2). From 12 to 24 h post naringenin addition, a decrease of fluorescence was observed in the BL21star™(DE3) host, while the MG1655(DE3) Δ*endA* Δ*recA* host showed a slight increase during the same period.

The performance of the different biosensors in M9 minimal media and a semi-rich defined media (AMM) was then evaluated and compared (Fig. 3). Contrary to expectations, *sgfp* was not overexpressed in semi-rich defined media, despite the advantage of rapid cell growth. Cells grown in AMM showed twice the OD_{600} but only about half the fluorescence signal of cells grown in M9 minimal media.

We constructed a dual-promoter system (Fig. 1A), with both the T7-lac promoter and the constitutive promoter BBa_J23113 upstream of the riboswitch. This system allowed us to switch transcription regulation depending on the presence of isopropyl β-D-1-thiogalactopyranoside (IPTG) in the media. In order to investigate the influence of different promoters, parallel experiments were performed with the aptamer-M1-based biosensor and 0.18 mM naringenin supplement at 5 h post inoculation. Fluorescence excitation was determined hourly by flow cytometry after induction. Selected results from the Fluorescence-Activated Cell Sorting (FACS)-generated histograms are shown in Figure 4A. The constitutive promoter controlled sensing-actuating components afforded stronger fluorescence excitation at 1 h post naringenin input (Fig. 4A blue histogram) than the T7-lac promoter (Fig. 4A orange histogram). Over the next 3 h, an equivalent fluorescent output was measured in both cases. However, the slight change in strength of system output suggests stronger control of the sensing-actuating components using the T7-lac promoter than the constitutive promoter-based system. The T7-lac promoter controlled sensor eventually, at 22 h, resulted in a very high fluorescent

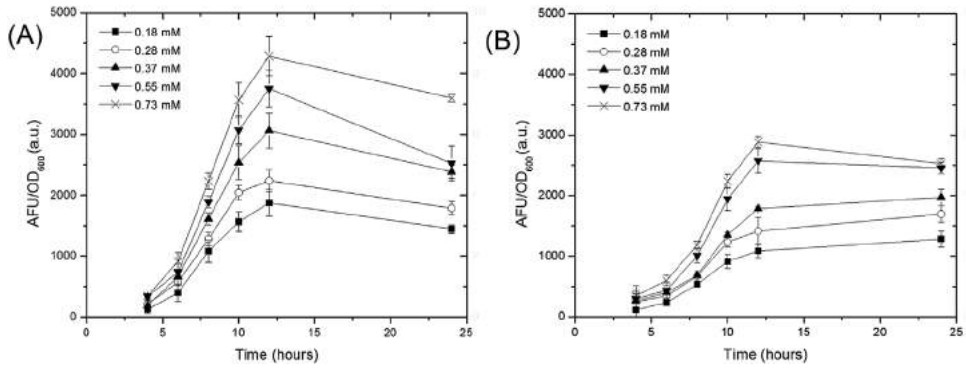

Figure 2. Fluorescence as a function of naringenin concentration via time. The aptamer-O-based biosensor was tested in two host strains (**A**) BL21star^{TM}(DE3) and (**B**) MG1655 (DE3) Δ*endA* Δ*recA* by time.

protein expression even though no naringenin was added to the culture, something that we interpreted as a false positive result.

Based on the previous observations, a constitutive promoter (BBa_J23113) controlled riboswitch biosensor device was re-constructed to avoid interference from IPTG in subsequent co-culture studies. When tested in shake flask cultures with naringenin added to the medium, the new device plasmid demonstrated a slightly increased dynamic range, from 4.55 (a.u.) in dual promoter device to 4.60 (a.u.) (Fig. 4B). Moreover, an empty pETM6 vector was transformed together with new biosensor device into BL21star^{TM}(DE3) to create a control strain that is resistant to both antibiotics, similarly to the naringenin producer strain. The resulting dynamic range of sensing-actuating device showed a decrease, to 4.52 (a.u.), in the control strain (Fig. 4B), while the EC_{50}, illustrated as dashed lines, was slightly increased in the control strain. Overall, the new device showed a relatively steady dynamic range and operational range when the additional plasmid was present.

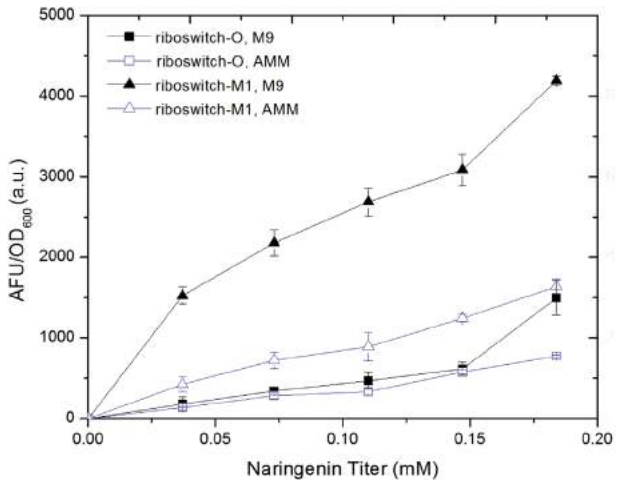

Figure 3. Effect of medium on biosensor performance. Aptamer-O-based biosensor and aptamer-M1-based biosensor, in BL21star^{TM}(DE3), were tested for their fluorescent response to different naringenin concentrations after growing for 19 h in M9 minimal media and AMM – 15g/L Glucose media, separately.

Quantification of In Vivo Metabolites in *E. coli* Co-Culture

A co-culture experiment with manual naringenin addition was performed in order to test the co-culture hypothesis while running a controlled pseudo-monoculture experiment (Fig. 5A). A consistent functional dependency between naringenin concentration (0.09 and 0.73 mM) in the medium and fluorescence shift assayed by FACS was found between both co-culture and pseudo-monoculture studies confirming the validity of the co-culture/sensor approach (Fig. 5B). Next, we validated the applicability of the constructed biosensor in measuring naringenin production levels by using our biosensor to monitor naringenin production from producer strains with different metabolic capabilities (Jones et al., 2016) (Fig. 6). All the constructed strains showed different naringenin productivities and a positive correlation between naringenin titer in co-culture and specific fluorescence of the sensor cells was demonstrated (Fig. 7). Only a small proportion (4% v/v) of the biosensor strain was required at inoculation to achieve an effective fluorescence excitation for screening.

Discussion

In this study, an RNA riboswitch-based biosensor was designed to respond to the flavanone naringenin (Fig. 1A). The biosensor displayed an increased fluorescent signal generation after activation of gene expression upon binding with naringenin, while in the absence of ligand, aptamer-mRNA formed a three-dimensional structure, preventing reporter gene expression. Mismatched regions (i.e., loops) in the mRNA play an important role in determining mRNA three-dimensional structures and can destabilize local structure. The structural change resulting from aptamer-ligand association, within mismatched regions, relies on its intermolecular interactions including stacking, electrostatic and hydrogen-bonding (Hermann and Patel, 2000; Kellenberger et al., 2015a; Wachsmuth et al., 2013; You et al., 2015). Thus, the aptamer portion is exploited as a core component of engineered riboswitches, since small nucleic acid

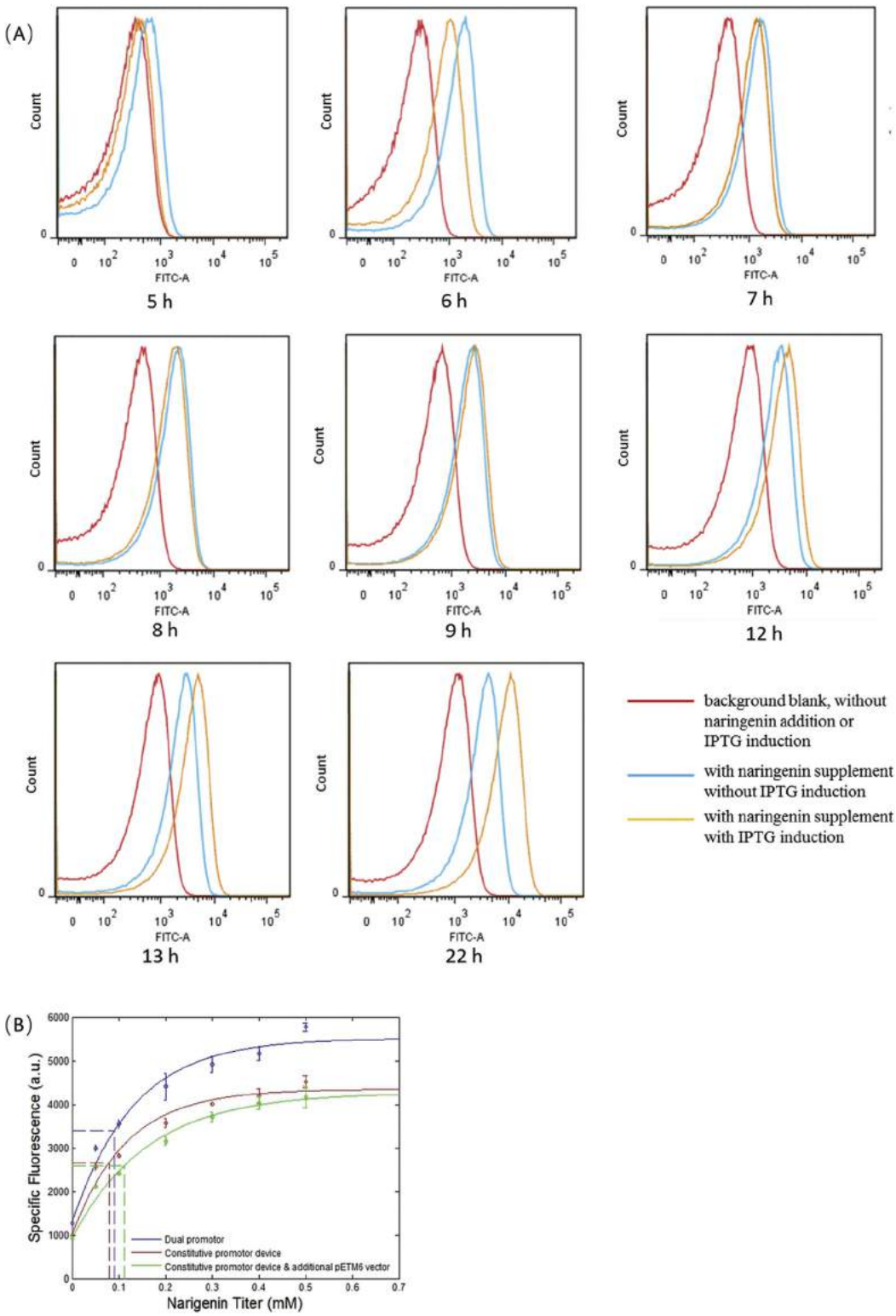

Figure 4. Fluorescent output in different promoter controlled biosensor via time. (**A**) The BL21star^{TM}(DE3) hosting the aptamer-M1-based biosensor where a dual-promoter was placed at the 5′-untranslated region of the sensing-actuation device. Naringenin addition or/and IPTG induction were made at 5 h after inoculation. The fluorescent intensity of a population of 100,000 cells for each case was examined by flow cytometry at different time points. (**B**) the dual-promoter was replaced by a constitutive promoter and the response of the new construct to naringenin was measured both with and without the empty vector plasmid pETM6. The EC_{50} for the different cases are illustrated as dashed lines.

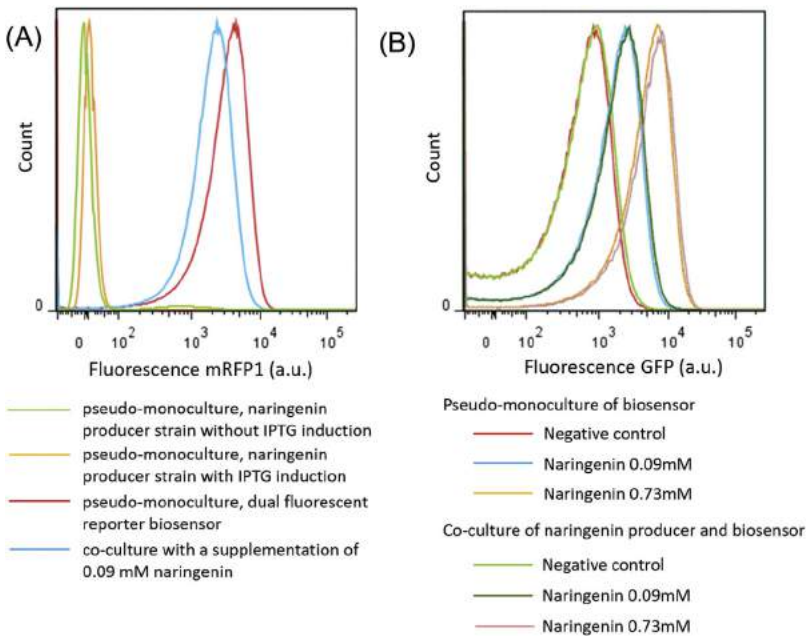

Figure 5. Dual-fluorescent response with naringenin in co-culture system. (**A**) The red fluorescence protein helped distinguish between naringenin and biosensor strain. (**B**) A comparison between pseudo-monoculture and co-culture system in response to the same naringenin concentration, 0.09 and 0.73 mM.

moieties are capable of determining the ligand binding affinity and specificity.

Naringenin plays a role as an inducer in this cell-based, sensing-actuating, genetically encoded biosensor. This way, the biosensor can "measure" the concentration of the intracellular or extracellular metabolite, and report it through the production of a fluorescent reporter protein, such as *sgfp*, providing a high-throughput screening method to detect differences in metabolic capabilities between strains. Any visible molecule or one that can alter cell fitness, such as the expression of an antibiotic resistance gene (Raman et al., 2014; Yang et al., 2013) or auxotrophic complements (Feng et al., 2015), can be employed in the expression module to facilitate efficient cycles of the design-build-test-learn loop. However, taking advantage of high throughput flow cytometry screening, one must face the drawback of overlapping fluorescence profiles that may lead to a high rate of false positives (Dietrich et al., 2010). Similarly, when the actuating

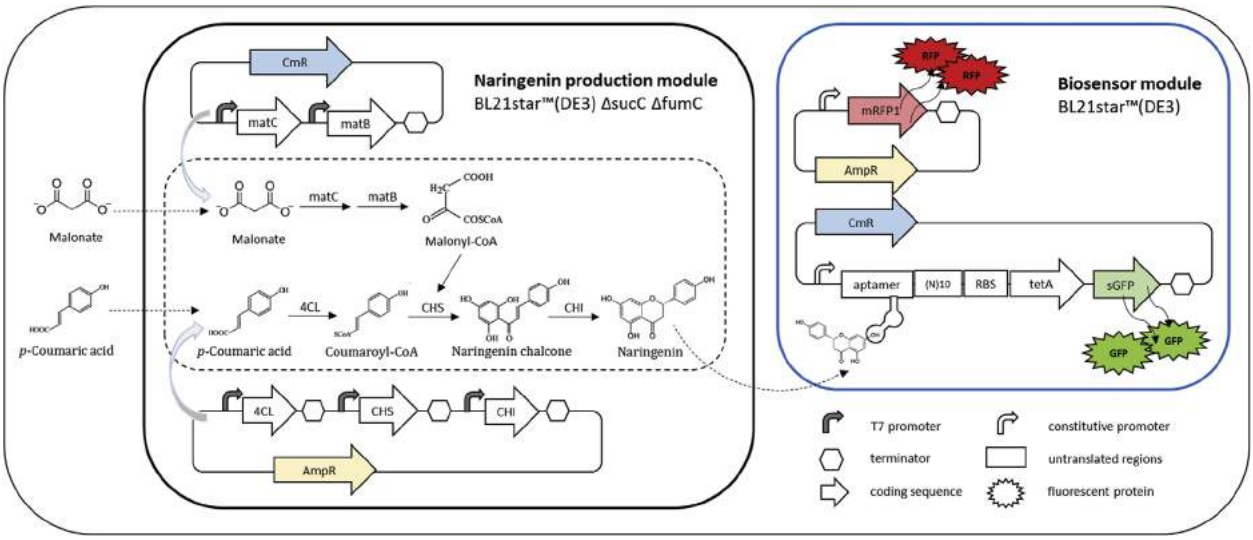

Figure 6. Schematic representation of biosensor-producer co-culture modules. The modified biosensor module carried both naringenin-responsive riboswitch-based green fluorescence device and constitutive red fluorescence device.

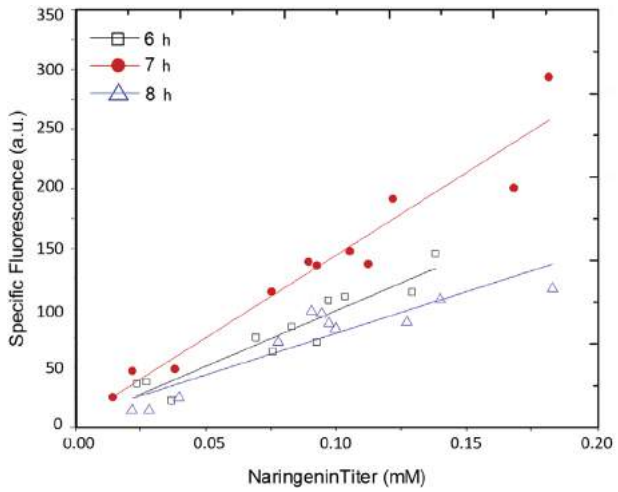

Figure 7. Correlation between naringenin produced and specific fluorescence. Strains with a range of naringenin production capabilities were grown in co-culture with the riboswitch-M1-based biosensor and induced with 1 mM IPTG at different time points (6, 7, or 8 h). Final fluorescence was measured by flow cytometry, while naringenin production was measured by HPLC. The coefficient of determination (R^2) was 0.8959, 0.9337, and 0.8415 for induction time points of 6, 7, and 8 h, respectively. Pearson's correlation coefficient (r^2) was calculated to be 0.9465, 0.9663, and 0.9173.

expression is a fitness advantage, cells that erroneously survive may take over the population (Rogers et al., 2016).

The fluorescence output of the biosensors was greatly influenced by a number of parameters, including the host strain and growth conditions such as media composition. This can be the result of metabolic burden that places hidden constraints on host cell productivity due to a high proportion of resources reassigned to expressing the recombinant pathway inside a host cell (Englaender et al., 2017; He et al., 2017; Wu et al., 2016). Although there are no common guidelines in place for how to regulate RNA device activities, the effect of some individual parameters such as host strain (Carothers et al., 2011) and observation time (Rogers et al., 2015) has been discussed in the literature. Based on our observations, BL21star^{TM}(DE3), M9 minimal media and harvest at 12 h post IPTG induction were chosen as the optimal conditions that ensure the compatibility of the RNA device in the host strain's background to create a riboswitch-based whole-cell biosensor.

Two key parameters impact the behavior of the riboswitch-based biosensor. First, the linkage $(N)_{10}$ between the aptamer and actuator, can dramatically impact the sensitivity and dynamic range of the biosensor (Fig. 1B,C). Similar results were reported to design a synthetic riboswitch (Win and Smolke, 2007; Yang et al., 2013; You et al., 2015). The principle for design mainly relies on the three-dimensional structure of the mRNA. Unfortunately, it is quite challenging to simulate a highly accurate three-dimensional mRNA structure, and predict the structural changes that accompany mRNA binding with the target small molecule. However, a framework for the modular assembly of aptamers, linkers and gene regulatory components, and some computational tools have been created to help with the design and prediction of RNA-based metabolite biosensors (Carothers et al., 2011; Endoh and Sugimoto, 2015; Espah Borujeni et al., 2016; Geertz et al., 2012; Townshend et al., 2015; Win and Smolke, 2007).

Second, the use of T7-lac promoter controlled aptamer-actuator biosensor (Fig. 1A) in the co-culture resulted in a significant naringenin-uninduced population that would complicate screening due to its strong IPTG-dependence (Fig. 4A). Thus, a constitutive promoter was employed for driving the expression of the aptamer-M1-based biosensor. This change of promoter did not influence biosensor dynamic and operational ranges (Figs. 4B and 5B). It was also reported that the gene expression noise can be reduced by switching to a constitutive promoter in the biosensor construction or decreasing plasmid copy number (Michener and Smolke, 2012).

The development of a biosensor assay in a co-culture application is then relatively straightforward (Fig. 6). A plasmid constitutively expressing an additional fluorescence marker, mRFP1, was introduced and applied to facilitate proper cell sorting using the FACS-based assay in the biosensor-producer co-culture. We showed that biosensor cell populations could be distinguished from other co-culture strains (Fig. 5). Two strains, BL21star^{TM}(DE3) (host of plasmid carrying the biosensor device) and BL21star^{TM}(DE3) Δ*sucC* Δ*fumC* (host of plasmid carrying the naringenin biosynthetic pathway), allow for relatively easy compatibility in the co-culture system (Fig. 6). It is important to note that there are three additional conditions that allowed us to use our biosensor device: First, the ability of target analyte, naringenin, to freely diffuse from the cell to the extracellular medium (Jones et al., 2016). Second, the specificity of the aptamer to bind to naringenin but not to precursor metabolite *p*-coumaric acid (data not shown). Third, the operational range of biosensor is similar to the cellular metabolite concentration (Siedler et al., 2014).

Hence, we were able to, for the first time, combine a riboswitch-based fluorescence biosensor strain and naringenin producing strain in co-culture for high throughout in vivo naringenin detection. The coefficient of determination (R^2) and Pearson's correlation coefficient (r^2) were calculated to measure how well the regression line approximates the actual data points and to measure the linear correlation between the HPLC and flow cytometry results (Fig. 7). This correlation critically relied on growth conditions, especially post-induction time. Under extended microbial co-culturing conditions, the biosensor is capable of not only distributing the metabolic burden and allowing module-specific optimization, it can also simplify library generation, screening, and selection, since removal of the biosensor strain will not influence metabolite production as is possible in a monoculture screening strategy.

Conclusions

In this work, an RNA riboswitch-based biosensor with dual fluorescence reporters was developed and applied to detect the in vivo production of naringenin through a novel co-culture approach using flow cytometry screening. This method is different from traditional monoculture-based sensors derived from transcription factors and can enable the design of high-throughput screening methods for metabolic engineering applications.

Materials and Methods

Bacterial Strains, Vectors, and Media

E. coli DH5α was used to propagate all plasmids. BL21star™(DE3) or MG1655(DE3) Δ*endA* Δ*recA* (Tseng et al., 2010), a gift from Kristala Prather (Addgene plasmid # 37854), was used as the host for RNA riboswitch vector. BL21star™(DE3) Δ*sucC* Δ*fumC* (Xu et al., 2011), with pETM6-xx4CL-xxCHS-xxCHI (The "xx" feature represents different homologs for each of the three enzymes from different plant sources) and pACYC-matC-matB, were used as naringenin production strains (Chemler et al., 2010; Jones et al., 2016). The vector pACYCDuet-1 was used as the basis for RNA riboswitch construction. A vector pYTK085 carrying mRFP1 gene (Lee et al., 2015), a gift from John Dueber (Addgene plasmid # 65192), was used directly as an extra fluorescent marker in co-culture biosensor. M9 salts (BD), Luria Broth (LB) lennox modification (Sigma) and semi-rich defined media (AMM) (He et al., 2015) were used where noted. All the nutrients and chemicals for medium preparation were purchased from Sigma–Aldrich (St. Louis, MO).

Sensor Component Construction

The naringenin riboswitch is comprised of an aptamer and expression platform (Fig. 1A). The aptamer was selected from in vitro selection using SELEX against a naringenin-coupled matrix, and the expression platform was evolved from in vivo dual selection(Yang et al., 2013): *tetA*, encoding a tetracycline/H^+ antiporter, and *sgfp*, encoding superfolder green fluorescent protein. A selecting $(N)_{10}$ and RBS was constructed as a functional actuator in between the aptamer and fusion protein gene. (Yang et al., 2013) The sequence of the riboswitches (O, M1, M2 and H2) tested in this paper are shown in Figure 1B. The riboswitch was under the control of a dual-promoter system consisting of an IPTG-inducible T7 promoter and a constitutive promoter (BBa_J23113) (Fig. 1A). Later, the device containing only the constitutive promoter was applied in the co-culture study.

Cultivation Protocol

Single colonies of each strain were inoculated separately into 10 mL of LB in a 125 mL non-baffled shake flask with corresponding antibiotics (ampicillin 80 μg/mL and/or chloramphenicol 25 μg/mL, as necessary) and grown overnight at 37 °C. After 14 h, the overnight culture was inoculated at 5% (100 μL) into 2 mL of M9 minimal media. The naringenin producer strain and biosensor strain co-culturing experiment utilized overnight cultures mixed before inoculation volumetrically to an indicated inoculation ratio of 25:1 (producer: biosensor). Naringenin was added to the desired final concentration at inoculation or as mentioned. After induced with 1 mM IPTG, the cultures were transferred to 30°C and allowed to grow for 12 h prior to analysis. All experiments were performed in polypropylene 48-well plates (5 mL, VWR). All the single-cell level experiments used M9 minimal medium with 4 g/L glucose, while the co-culture experiments used M9 minimal medium with 15 g/L glucose. Sodium malonate (1 g/L, Sigma) and *p*-coumaric acid (50 mg/L, Sigma) were added at induction as substrates for naringenin production.

Metabolic Analysis

The supernatant (25 μL) of fermentation broth obtained through centrifugation (2 min, 20,000*g*) was used for HPLC analysis, which was carried out using Agilent 1200 series HPLC (Santa Clara, CA) equipped with a ZORBAX SB-18 column (5 μm, 4.6 × 150 mm) and a diode array detector. The mobile phase was acetonitrile (solvent A) and water (solvent B) (both contained 0.1% formic acid) was used at a flow rate of 1 mL/min. The HPLC program was 10–40% A (0–10 min) and 40–60% A (10–15 min) (Jones et al., 2016; Zhao et al., 2015). Absorbance at 280 nm was monitored in all cases. Naringenin standard was purchased from Sigma–Aldrich and was dissolved in pure ethanol.

Florescence Assay

Endpoint green fluorescence (excitation wavelength of 485 nm and emission wavelength of 535 nm) and OD_{600} measurements were obtained in 96-well black, clear bottom plates (Nunc Products, Rochester, NY) on a Biotek Synergy 4 instrument (Winooski, VT). The ratio of fluorescence to absorbance at 600 nm (AFU/OD_{600}, given in a.u.) was used to compensate for changes in cell density over time and between experiments. Cultures were diluted into the linear range as necessary.

Flow cytometry was performed on LSRII flow cytometer (BD Biosciences, San Jose, CA) with 488 nm excitation from a blue solid-state laser for all the co-culture experiments. Fluorescence was detected using a 505-nm long-pass and a 530/30-nm band-pass filter set for *sgfp*, or 600-nm long-pass and a 610/20-nm band-pass filter set for mRFP1, respectively. Cells collected with centrifugation (2 min, 20,000*g*) were washed and diluted in cold phosphate buffered saline (PBS) and kept on ice until evaluation. Gating was performed on forward and side scatter to avoid debris and clumped cells, then on mRFP1 to avoid background from producer strain, by using BD FACSDiVa 7.0 software. The specific fluorescence was defined as the value of geometric fluorescence mean of 100,000 cells (given in a.u.).

A control sample, of only one strain and without naringenin or inducer addition was performed in all experiments as a background blank. The specific background fluorescence value was subtracted to ensure it was comparable between each biosensor. All experiments were performed in triplicates. Error bars represent ± 1 standard deviation of biological triplicates.

Authors' Contributions

Y.X., M.A.G.K., and G.Y.J. designed the study. Y.X., Q.P.Y., J.A.J., and R.J.L. analyzed the data and wrote the manuscript. S. J. performed the SELEX and constructed the dual-promoter riboswitch-based device plasmid. Y.X. performed all the other experiments with assistance and advice from J.A.J. and N.A.Z.

This work was supported by the National Natural Science Foundation of China (grant number 21376017) and the RPI Biocatalysts and Metabolic

Engineering Constellation Fund. This work was also supported by the National Research Foundation of Korea (NRF) grant (NRF-2016K1A1A2912829, NRF-2015R1A2A1A10056126) funded by the Korea government (Ministry of Science, ICT & Future Planning). The authors would like to thank Dr. Sergey Pryshchep, Dr. Paiyz Mikael, and Matthew Brier for assistance and suggestions regarding flow cytometry experiments, and Dr. Brady F. Cress for critical discussions.

References

Alam KK, Chang JL, Burke DH. 2015. FASTAptamer: A bioinformatic toolkit for high-throughput sequence analysis of combinatorial selections. Mol Ther Acids 4: e230.

Beisel CL, Chen YY, Culler SJ, Hoff KG, Smolke CD. 2011. Design of small molecule-responsive microRNAs based on structural requirements for Drosha processing. Nucleic Acids Res 39(7):2981–2994.

Bhan N, Xu P, Koffas MAG. 2013. Pathway and protein engineering approaches to produce novel and commodity small molecules. Curr Opin Biotechnol 24(6):1137–1143.

Bloom RJ, Winkler SM, Smolke CD. 2014. A quantitative framework for the forward design of synthetic miRNA circuits. Nat Methods 11(11):1147–1153.

Carothers JM, Goler JA, Juminaga D, Keasling JD. 2011. Model-driven engineering of RNA devices to quantitatively program gene expression. Science 334(6063):1716–1719.

Chang AL, Wolf JJ, Smolke CD. 2012. Synthetic RNA switches as a tool for temporal and spatial control over gene expression. Curr Opin Biotechnol 23(5):679–688.

Chemler JA, Fowler ZL, McHugh KP, Koffas MAG. 2010. Improving NADPH availability for natural product biosynthesis in *Escherichia coli* by metabolic engineering. Metab Eng 12(2):96–104.

Cress BF, Trantas EA, Ververidis F, Linhardt RJ, Koffas MAG. 2015. Sensitive cells: Enabling tools for static and dynamic control of microbial metabolic pathways. Curr Opin Biotechnol 36:205–214.

Cress BF, Jones JA, Kim DC, Leitz QD, Englaender JA, Collins SM, Linhardt RJ, Koffas MAG. 2016. Rapid generation of CRISPR/dCas9-regulated, orthogonally repressible hybrid T7-lac promoters for modular, tuneable control of metabolic pathway fluxes in *Escherichia coli*. Nucleic Acids Res 44(9):4472–4485.

Davydova A, Vorobjeva M, Pyshnyi D, Altman S, Vlassov V, Venyaminova A. 2016. Aptamers against pathogenic microorganisms. Crit Rev Microbiol 42(6):1–19.

Dietrich JA, McKee AE, Keasling JD. 2010. High-throughput metabolic engineering: Advances in small-molecule screening and selection. Annu Rev Biochem 79(1):563–590.

Dixon N, Duncan JN, Geerlings T, Dunstan MS, McCarthy JEG, Leys D, Micklefield J. 2010. Reengineering orthogonally selective riboswitches. Proc Natl Acad Sci U S A 107(7):2830–2835.

Endoh T, Sugimoto N. 2015. Rational design and tuning of functional RNA switch to control an allosteric intermolecular interaction. Anal Chem 87(15):7628–7635.

Englaender JA, Jones JA, Cress BF, Kuhlman TE, Linhardt RJ, Koffas MAG. 2017. Effect of genomic integration location on heterologous protein expression and metabolic engineering in *E. coli*. ACS Synth Biol. 6(4):710–720.

Espah Borujeni A, Mishler DM, Wang J, Huso W, Salis HM. 2016. Automated physics-based design of synthetic riboswitches from diverse RNA aptamers. Nucleic Acids Res 44(1):1–13.

Feng J, Jester BW, Tinberg CE, Mandell DJ, Antunes MS, Chari R, Morey KJ, Rios X, Medford JI, Church GM, Fields S, Baker D. 2015. A general strategy to construct small molecule biosensors in eukaryotes. eLife 4:1–23.

Geertz M, Shore D, Maerkl SJ. 2012. Massively parallel measurements of molecular interaction kinetics on a microfluidic platform. Proc Natl Acad Sci U S A 109(41):16540–16545.

He W, Fu L, Li G, Jones JA, Linhardt RJ, Koffas MAG. 2015. Production of chondroitin in metabolically engineered *E. coli*. Metab Eng 27:92–100.

He L, Xiu Y, Jones JA, Baidoo EEK, Keasling JD, Tang YJ, Koffas MAG. 2017. Deciphering flux adjustments of engineered *E. coli* cells during fermentation with changing growth conditions. Metab Eng 39:247–256.

Hermann T, Patel DJ. 2000. Adaptive recognition by nucleic acid aptamers. Science 287(5454):820–825.

Hoinka J, Berezhnoy A, Dao P, Sauna ZE, Gilboa E, Przytycka TM. 2015. Large scale analysis of the mutational landscape in HT-SELEX improves aptamer discovery. Nucleic Acids Res 43(12):5699–5707.

Jones JA, Vernacchio VR, Sinkoe AL, Collins SM, Ibrahim MHA, Lachance DM, Hahn J, Koffas MAG. 2016. Experimental and computational optimization of an *Escherichia coli* co-culture for the efficient production of flavonoids. Metab Eng 35:55–63.

Kellenberger CA, Chen C, Whiteley AT, Portnoy DA, Hammond MC. 2015a. RNA-based fluorescent biosensors for live cell imaging of second messenger cyclic di-AMP. J Am Chem Soc 137(20):6432–6435.

Kellenberger CA, Sales-Lee J, Pan Y, Gassaway MM, Herr AE, Hammond MC. 2015b. A minimalist biosensor: Quantitation of cyclic Di-GMP using the conformational change of a riboswitch aptamer. RNA Biol 12:1189–1197.

Lee SW, Oh MK. 2015. A synthetic suicide riboswitch for the high-throughput screening of metabolite production in *Saccharomyces cerevisiae*. Metab Eng 28:143–150.

Lee ME, DeLoache WC, Cervantes B, Dueber JE. 2015. A highly characterized yeast toolkit for modular, multipart assembly. ACS Synth Biol 4(9):975–986.

Lee CH, Han SR, Lee S-W. 2016. Therapeutic applications of aptamer-based riboswitches. Nucleic Acid Ther 26(1):44–51.

Liu D, Evans T, Zhang F. 2015. Applications and advances of metabolite biosensors for metabolic engineering. Metab Eng 31:35–43.

Lynch SA, Desai SK, Sajja HK, Gallivan JP. 2007. A High-throughput screen for synthetic riboswitches reveals mechanistic insights into their function. Chem Biol 14(2):173–184.

Marin AM, Souza EM, Pedrosa FO, Souza LM, Sassaki GL, Baura VA, Yates MG, Wassem MG, Monteiro RA. 2013. Naringenin degradation by the endophytic diazotroph Herbaspirillum seropedicae SmR1. Microbiol (United Kingdom) 159(1):167–175.

McKeague M, Wong RS, Smolke CD. 2016. Opportunities in the design and application of RNA for gene expression control. Nucleic Acids Res 44(7):2987–2999.

Meyer A, Pellaux R, Potot S, Becker K, Hohmann HP, Panke S, Held M. 2015. Optimization of a whole-cell biocatalyst by employing genetically encoded product sensors inside nanolitre reactors. Nat Chem 7(8):673–678.

Michener JK, Smolke CD. 2012. High-throughput enzyme evolution in *Saccharomyces cerevisiae* using a synthetic RNA switch. Metab Eng 14(4):306–316.

Paige JS, Nguyen-Duc T, Song W, Jaffrey SR. 2012. Fluorescence imaging of cellular metabolites with RNA. Science 335(6073):1194.

Pandey RP, Parajuli P, Koffas MAG, Sohng JK. 2016. Microbial production of natural and non-natural flavonoids: Pathway engineering, directed evolution and systems/synthetic biology. Biotechnol Adv 34(5):634–662.

Raman S, Rogers JK, Taylor ND, Church GM. 2014. Evolution-guided optimization of biosynthetic pathways. Proc Natl Acad Sci U S A 111(50):17803–17808.

Rogers JK, Guzman CD, Taylor ND, Raman S, Anderson K, Church GM. 2015. Synthetic biosensors for precise gene control and real-time monitoring of metabolites. Nucleic Acids Res 43(15):7648–7660.

Rogers JK, Taylor ND, Church GM. 2016. Biosensor-based engineering of biosynthetic pathways. Curr Opin Biotechnol 42:84–91.

Siedler S, Stahlhut SG, Malla S, Maury J, Neves AR. 2014. Novel biosensors based on flavonoid-responsive transcriptional regulators introduced into *Escherichia coli*. Metab Eng 21:2–8.

Terán W, Felipe A, Segura A, Rojas A, Ramos J-L, Gallegos M-T. 2003. Antibiotic dependent induction of *Pseudomonas putida* DOT-T1E TtgABC efflux pump is mediated by the drug binding repressor TtgR. Antimicrob Agents Chrmotherapy 47(10):3067–3072.

Thaiss CA, Itav S, Rothschild D, Meijer MT, Levy M, Moresi C, Dohnalová L, Braverman S, Rozin S, Malitsky S, Bachash MD, Kuperman Y, Biton I, Gertler A, Harmelin A, Shapiro H, Halpern Z, Aharoni A, Segal E, Elinav E. 2016. Persistent microbiome alterations modulate the rate of post-dieting weight regain. Nature 540(7634):1–27.

Topp S, Gallivan JP. 2010. Emerging applications of riboswitches in chemical biology. ACS Chem Biol 5(1):139–148.

Topp S, Reynoso CMK, Seeliger JC, Goldlust IS, Desai SK, Murat D, Shen A, Puri AW, Komeili A, Bertozzi CR, Scott JR, Gallivan JP. 2010. Synthetic riboswitches that induce gene expression in diverse bacterial species. Appl Environ Microbiol 76(23):7881–7884.

Townshend B, Kennedy AB, Xiang JS, Smolke CD. 2015. High-throughput cellular RNA device engineering. Nat Methods 12(10):989–994.

Trausch JJ, Ceres P, Reyes FE, Batey RT. 2011. The structure of a tetrahydrofolate-sensing riboswitch reveals two ligand binding sites in a single aptamer. Structure 19(10):1413–1423.

Tseng H-C, Harwell CL, Martin CH, Prather KLJ. 2010. Biosynthesis of chiral 3-hydroxyvalerate from single propionate-unrelated carbon sources in metabolically engineered *E. coli*. Microb Cell Fact 9(1):96.

Wachsmuth M, Findeiß S, Weissheimer N, Stadler PF, Mörl M. 2013. De novo design of a synthetic riboswitch that regulates transcription termination. Nucleic Acids Res 41(4):2541–2551.

Wang J, Guleria S, Koffas MAG, Yan Y. 2016. Microbial production of value-added nutraceuticals. Curr Opin Biotechnol 37:97–104.

Weigand JE, Suess B. 2007. Tetracycline aptamer-controlled regulation of pre-mRNA splicing in yeast. Nucleic Acids Res 35(12):4179–4185.

Win MN, Smolke CD. 2007. A modular and extensible RNA-based gene-regulatory platform for engineering cellular function. Proc Natl Acad Sci U S A 104(36):14283–14288.

Wittmann A, Suess B. 2012. Engineered riboswitches: Expanding researchers' toolbox with synthetic RNA regulators. FEBS Lett 586(15):2076–2083.

Wu G, Yan Q, Jones JA, Tang YJ, Fong SS, Koffas MAG. 2016. Metabolic burden: Cornerstones in synthetic biology and metabolic engineering applications. Trends Biotechnol 34(8):652–664.

Xu P, Ranganathan S, Fowler ZL, Maranas CD, Koffas MAG. 2011. Genome-scale metabolic network modeling results in minimal interventions that cooperatively force carbon flux towards malonyl-CoA. Metab Eng 13(5):578–587.

Yang J, Seo SW, Jang S, Shin SI, Lim CH, Roh TY, Jung GY. 2013. Synthetic RNA devices to expedite the evolution of metabolite-producing microbes. Nat Commun 4:1413.

You M, Litke JL, Jaffrey SR. 2015. Imaging metabolite dynamics in living cells using a Spinach-based riboswitch. Proc Natl Acad Sci U S A 112(21):E2756–E2765.

Zhao S, Jones JA, Lachance DM, Bhan N, Khalidi O, Venkataraman S, Wang Z, Koffas MAG. 2015. Improvement of catechin production in *Escherichia coli* through combinatorial metabolic engineering. Metab Eng 28:43–53.

Zhou LB, Zeng AP. 2015. Exploring lysine riboswitch for metabolic flux control and improvement of L-lysine synthesis in corynebacterium glutamicum. ACS Synth Biol 4(6):729–734.